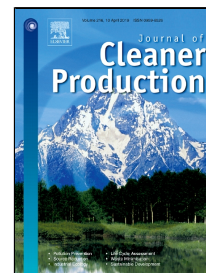


# Accepted Manuscript

Environmental burdens of groundwater extraction for irrigation over an inland river basin in Northwest China



Jun Niu, Xin-Guang Zhu, Martin A.J. Parry, Shaozhong Kang, Taisheng Du, Ling Tong, Risheng Ding

PII: S0959-6526(19)30766-8  
DOI: 10.1016/j.jclepro.2019.03.075  
Reference: JCLP 16079  
To appear in: *Journal of Cleaner Production*  
Received Date: 28 August 2017  
Accepted Date: 07 March 2019

Please cite this article as: Jun Niu, Xin-Guang Zhu, Martin A.J. Parry, Shaozhong Kang, Taisheng Du, Ling Tong, Risheng Ding, Environmental burdens of groundwater extraction for irrigation over an inland river basin in Northwest China, *Journal of Cleaner Production* (2019), doi: 10.1016/j.jclepro.2019.03.075

This is a PDF file of an unedited manuscript that has been accepted for publication. As a service to our customers we are providing this early version of the manuscript. The manuscript will undergo copyediting, typesetting, and review of the resulting proof before it is published in its final form. Please note that during the production process errors may be discovered which could affect the content, and all legal disclaimers that apply to the journal pertain.

# Environmental burdens of groundwater extraction for irrigation over an inland river basin in Northwest China

Jun Niu<sup>a\*</sup>, Xin-Guang Zhu<sup>b</sup>, Martin A.J. Parry<sup>c</sup>, Shaozhong Kang<sup>a\*\*</sup>, Taisheng Du<sup>a</sup>, Ling Tong<sup>a</sup>, Risheng Ding<sup>a</sup>

<sup>a</sup>Center for Agricultural Water Research in China, China Agricultural University, Beijing 100083, China.

<sup>b</sup>CAS Key laboratory for Computational Biology and State Key Laboratory for Hybrid Rice, CAS-MPG Partner Institute for Computational Biology, Chinese Academy of Sciences, Shanghai 200000, China.

<sup>c</sup>Lancaster Environment Centre, Lancaster University, Bailrigg, Lancaster LA1, 4YQ, UK.

\*Correspondence author.

E-mail address: niuj@cau.edu.cn (J. Niu), kangsz@cau.edu.cn (S.Z. Kang)

## Abstract

Crop production is expected to increase by more than 50% to meet the demand of population growth in China in 2050 (FAO, 2017). Crop production in North China largely depends on irrigation, which is mainly from groundwater in Northwest China. Over-extraction of groundwater is decreasing groundwater levels, and threatening the fragile ecological systems of arid regions. How groundwater levels will change in order to meet the irrigation water requirement in Northwest China has not been extensively investigated to evaluate sustainability of agriculture and the cost to maintain groundwater levels. Here, we examine the dynamic relations between groundwater levels and the amount of irrigation water, by employing the Variable Infiltration Capacity model and an irrigation scheme, for the last three decades in Heihe River basin of China. The results show that on the average about 1.86 m decline of groundwater is attributable to the irrigation water consumption for the farmland area in Heihe River over the past three decades. In the scenario of ceasing irrigation activities, the groundwater level will be prevented to further decline about

3.06±0.4m under the future climate scenarios till 2050, but at the cost of crop production valued 64.2±8.4 billion CNY. Effective water-saving measures and strategies are expected to adopt to maintain both groundwater levels and agricultural productivity for the coming decades.

**Keywords:** Irrigation; Evapotranspiration; Crop production; Groundwater level; Northwest China

## 1. Introduction

The increasing food demand due to population growth has forced agriculture to both expand and intensify over the past several decades (Shiklomanov and Rodda, 2003; Molden et al., 2007; Wu et al., 2015). For the regions with limited precipitation, future increase in crop production must rely on irrigation (You et al., 2014). Groundwater is a critical and increasingly important source of irrigation water in China (Grogan et al., 2015) and globally, such as the Northwest India Aquifer (Rodell et al., 2009), US High Plain (Scanlon et al., 2012), California's Central Valley (Famiglietti et al., 2011), and North China Plain (Feng et al., 2013). In the past 50 years, Agriculture in China expanded significantly and now over 50% of national crop production comes from the dry region of Northern China (Calow et al., 2009). Since 1970, over 40% of irrigation water used for crop production has been groundwater (Currell et al., 2012; Cao et al., 2013). Consequently the groundwater levels (GWL) in the North China Plain have dropped by 15m since 1960, currently decreasing at the rate of about 1m/year regionally. For the water-scarce region in Northwest China, where agriculture heavily relies on groundwater, more attentions are needed for both ensuring crop production and protecting the vulnerable ecological conditions (Kang et

al., 2004).

Grogan et al. (2015) provided a valuable study on the link between irrigation water demand and mined groundwater in China based on 0.5 degree grid cells. The goal of this study is to understand how the groundwater resources have been affected by human interventions and climate evolutions both historically (1981-2010) and in the next 30-year period. Specifically, we focus on the oasis region in the Heihe River basin (Fig.1) based on 0.125 degree grid cells, which is a typical arid basin in Northwest China, with 3 million square kilometers and it has been experiencing typical GWL declines. We aim to quantify how much effort or cost we need to pay for recovering/preventing the groundwater declines in this region. This study sheds light on future evolutions of the ecological conditions in terms of the groundwater declines in Northwest China.

## 2. Study area and data

The Heihe River basin is the second largest inland river basin in China. It is a typical arid and semiarid river basin in Northwest China (Fig. 1). The upper reach of the basin is the Qilian Mountain area, which is a main runoff generation area by both precipitation and snowmelt water. It produces about  $2.22 \times 10^9 \text{m}^3/\text{year}$  of surface water during the period of 2000-2008, and about  $1.72 \times 10^9 \text{m}^3/\text{year}$  flows through Yingluoxia to the middle reach of the basin (Wu et al., 2014). The middle reach of the basin (MH), through which is the famous Silk Road, includes a large area of alluvial fans and floodplains, and has intensively irrigated farmlands in its oasis. The annual average temperature is about  $5.2 \text{ }^\circ \text{C}$ , and the annual precipitation varies in space

from 50-400mm, with an average of 145mm. The main crops are maize, winter-wheat, and cabbage. The agricultural water consumption reaches about  $1.89 \times 10^9 \text{m}^3/\text{year}$  for the period of 2000-2008 (Zhangye-MY, 2010; Wu et al., 2014). Zou et al. (2018) estimated irrigation water requirement for the period of 2001-2010 is about  $2.1 \times 10^9 \text{m}^3/\text{year}$ . The irrigated water, apart from diverting from surface water, is pumped from the groundwater for the crop irrigation. The local water resources is mostly consumed/transformed in UMH (the upper and middle reaches), which is focused in this study.

[Please insert Figure 1 here]

There are 5 meteorological stations in UMH. These 5 observations are not sufficient for the 276 grid cells we studied with the spatial resolution of 1/8 degree. A regional climate model, Regional Integrated Environmental Model System (RIEM2.0), which was well calibrated with both ground observations and remote sensing data, is available for the Heihe River basin (Xiong and Yan, 2013). The products provide the meteorological inputs, including precipitation, maximum and minimum temperatures, relative humidity, wind speed, and wind direction data, with a high spatial resolution ( $3\text{km} \times 3\text{km}$  grids) at the time step of 6 hours. Given the less uncertainty of the physical-based modelling and more information sources incorporated, the model-derived data were used for VIC modeling in our study. These data were aggregated into the spatial resolution of 1/8 degree with the time step of daily for the VIC model simulation. Topography and land cover classification (vegetation and soil parameters) for non-irrigated area were extracted from global

datasets with a  $0.5^{\circ} \times 0.5^{\circ}$  spatial resolution as described in Nijssen et al. (2001). For the irrigated area, the crop types, crop Leaf Area Index (LAI), and cropping intensity are found in FAO' database (FAO, 2003) and the Cold and Arid Regions Science Data Center, Chinese Academy of Science, (<http://westdc.westgis.ac.cn>). The fraction of area irrigated within each grid cell was derived from land use map in 2000 (Portmann et al., 2010). Monthly diversion and pumping data of the irrigation districts were obtained from local water resources authorities (Zhangye-MY, 2010). The RCP projections are derived from the model HadGEM2-ES (Hadley Centre Global Environment Model version 2-Earth System) (Collins et al., 2008), which has been further downscaled into the spatial resolution of  $0.5^{\circ} \times 0.5^{\circ}$  from initial  $1.875^{\circ} \times 1.25^{\circ}$  by using the correction and interpolation methods in ISI-MIP (Inter-Sectoral Impact Model Intercomparison Project).

### 3. Methods

#### 3.1 Hydrological modelling

The macroscale hydrological model in this study is the grid-based Variable Infiltration Capacity (VIC) model (Liang et al., 1994), which solves the water and energy balance equations at the land surface (Lakshmi et al., 2004). Each grid cell, usually implemented at spatial scales from  $1/8$  to  $2$  latitude by longitude, is partitioned into multiple vegetation types (and bare soil), and the soil column is divided into multiple (typically three) soil layers. The hydrological response of large areas is represented through the parameterization of the partitioning of precipitation into direct runoff and infiltration (Zhao et al., 1980), and the nonlinear effects of baseflow depending on

subsurface soil storage (Todini, 1996). Evapotranspiration is calculated using the Penman-Monteith equation (Shuttleworth, 1993). Surface runoff and baseflow are routed from each grid cell to the basin outlet through a triangular unit hydrograph and the linearized Saint-Venant equation via river network (Lohmann et al., 1996). More details of the relevant algorithms are described in Liang et al. (1994). The VIC model was modified to allow for irrigation water use based on the predicted soil moisture deficit in the model using an irrigation scheme described by Haddeland et al. (2006). Each Grid cell is partitioned into an irrigated and a non-irrigated part. Using the VIC hydrological model including the infiltration, surface runoff, subsurface runoff, drainage from the soil layer, and irrigation scheme, together with accurate geophysical, geological and meteorological forcing datasets, we carried out the hydrological simulation based on model calibrations. The VIC model application with both water and energy modes is more reasonable to quantify the irrigation water requirement for a large-scale agricultural land (Tatsumi and Yamashiki, 2015). For more efficient implementation, the Particle Swarm Optimization (PSO) (Shi and Eberhart, 1998) was selected to perform the parameter optimization. To evaluate the model performance for the calibration and validation periods, two common criteria, Coefficient of Determination ( $R^2$ ) and Nash-Sutcliffe efficiency (NSE) were used.

### 3.2 Irrigation water requirement

Irrigation starts when soil moisture drops down to the level below which transpiration becomes limited, and continues until soil moisture reaches field capacity. The water from surface runoff, river channels, dams, and groundwater extraction are considered

for the irrigation water withdrawals until water levels reaches the required for optimal crop growth. The net irrigation water requirement (NIWR) is calculated as the quantity of freely available water that is necessary to maintain the crop growth for the sustained agricultural production (Frenken and Gillet, 2012; Tatsumi et al, 2011). The NIWR is estimated for the irrigated area in each grid cell on the basis of the irrigation requirement. In this study, the NIWR is proposed as follows:

$$NIWR = \frac{\sum_{i=1}^N \sum_{t=1}^T (k_{ct} \times ET_{0t} - ET_{nt}) \times A_i}{A} \quad (1)$$

where NIWR is the annual net irrigation water requirement (mm),  $i$  is the number of given crops with  $N$  types,  $t$  is the growth stage and  $T$  is the total stages,  $k_c$  is the crop coefficient, varied with each crop and growth stage,  $ET_0$  is the reference evapotranspiration rate calculated by a Penman-Monteith formulation,  $ET_n$  is the natural evapotranspiration with only available rainfall for different growth stage and no irrigation,  $A_i$  is the area cultivated with crop  $i$  and  $A$  is the total cultivated area.

Meanwhile, the NIWR, empirically is also a function of irrigation efficiency ( $I_{eff}$ ), irrigation water extractions (IWE), and the proportion of water withdrawals between surface water and groundwater ( $P_{sg}$ ):

$$NIWR = f(I_{eff}, P_{sg}, IWE) \quad (2)$$

The IWE here is not only for the irrigation purpose, but also for domestic water use, industrial water use, and ecological water requirement. However, the large proportion of IWE is used for irrigation water, accounted for over 85% of the total water use on the average, over the middle reach of the Heihe River basin we studied. Combined

Equation (1) and (2), the value of IWE and groundwater level (GWL) changes can be inverted. Based on the above methods, the frame diagram of the proposed study is shown in Figure 2.

[Please insert Figure 2 here]

## 4. Results

### 4.1 Model evaluation

Monthly discharge data before the operation of the reservoir (in 2000) at the Yingluoxia station (see Fig.1f) is mainly used for calibration and validation of the natural runoff generation and routing processes of the VIC model. The comparison of the monthly streamflow variability between observations and simulations by the VIC model demonstrated satisfied model performance, as shown in Figure 3. For example, the  $R^2$  varied from 0.754 and 0.719 during both calibration and validation periods, with NSE of 0.699 and 0.675 respectively. The ET data set, derived from remote sensing product, was employed to validate the ET simulation in the irrigated area. The comparisons between the monthly grid-based ET estimated by the VIC model with incorporating irrigation scheme and that calculated based on remote sensing data, for Site C and D, as shown in Figure 4, indicated that simulations were in a good agreement with the remote sensing derived data. For the ET examined,  $R^2$ /NSE value is 0.739/0.782 and 0.777/0.789, for Site C and D, respectively. Note that the ET validation involve the assumptions that the crops are freely irrigated and the optimal crop growth are achieved. In addition, the water level observations at 31 monitoring wells were used to further check the net irrigation water requirement we estimated.

Overall, the spatial comparison and statistical measures on both streamflow and evapotranspiration simulations were in good agreement with the observations for the hydrological processes in agricultural lands.

[Please insert Figure 3–4 here]

#### 4.2 Net irrigation water requirement

Figure 1c shows the spatial features of rain-fed evapotranspiration (ET), when no human activities are assumed in the upper and middle reaches of the Heihe River basin (UMH). The annual average ET for the period of 1981-2010 is less than 450 mm/year. The ET distribution under free irrigation is displayed in Fig. 1d, which significantly increases the local ET amount for the farmland area in the middle reach of the Heihe basin (MH), with maximum value approaching 700 mm/year. The water in the free irrigation is assumed to be freely available (Haddeland et al., 2006). Figure 1(e) shows the ET differences between the rain-fed and free-irrigated processes, which demonstrates that the irrigation water withdrawal leads to increased ET in MH. The differences are the net irrigation water requirement for maintaining the crop growth in the region. It is observed that the region where irrigation is needed is isolated from rain-fed processes (Fig. 1c). The region is essentially flat oasis area in the front of the mountain area, which is the part of the Hexi Corridor in Northwest China. Among the identified grid cells with ET differences, the grids with high value of net irrigation water requirement are not only close to the river, but also located in the western and eastern parts, which indicates the necessity of extracting groundwater to meet the irrigation water demand.

#### 4.3 Groundwater level (GWL) changes

The net irrigation water requirement revealed in Figure 1 need to be satisfied to maintain the crop growth. Figure 5 shows the temporal variations of both rain-fed ET and free-irrigated ET at Site A (see. Fig.1b) during the period of 1990-2010 in the basin. It is observed that all rain-fed ET is less than the free-irrigated, which indicates that the water is insufficient for the crop growth during this period. The large differences, such as year 1990, 1995, and 2001, demonstrates the large requirements due to the precipitation deficit in these years. As a part of these requirements relied on the groundwater extraction, we derived the GWL changes according to the temporal net irrigation water requirement at the site using Equations (1-2). The abrupt change of GWL corresponds to the large differences between rain-fed ET and free-irrigated ET. During the period of 1990-2010, the GWL declined from about 1392m to 1391m, with the annual decline rate of 0.05m/year for Site A.

[Please insert Figure 5 here]

Figure 6(a) summarizes the monthly water level variations of the observed wells in Linze district in MH, among which only 9 wells have continuous records for the period 1990-2004, and a decline trend is shown in the left panel of the Figure. The right panel of Fig. 6a shows the changes of GWL during 1990-2004 for the Linze district ranging from -2m to 0.5m. The average value of inverted GWL changes over the district was estimated to be 0.7m, which is close to the medium value of the observed wells. Please note that the boxplot in the right panel is based on the observations of 15 wells; while for the other 6 wells, the record is continuous for the

period of 1990-2004. The GWL decline in Ganzhou district was much higher than that in the Linze district, with the maximum decline of 9.6m, as shown in Fig. 6b. The decline trend is more significant during the latter years. The inverted GWL estimated was about -1.9m, which is also close to the medium value of the 15 wells in this district. There are some newly drilled wells for the Linze and Ganzhou districts, as shown in Fig. 1f. Most of them have the continuous records for the period of 2000-2010. For the 10 wells in Linze district, the inverted GWL estimated was -0.94m, and the medium value of the 10 wells is -1.01m, as shown in Fig. 7. The inverted GWL estimated for Ganzhou district is -0.74, which is close to the medium value of the observed wells. The consistency between the inverted GWL changes and observed well changes is not great for the period of 2000-2010, as compared to that of 1990-2004. This is possibly attributed to the different locations of the observed wells, as the newly drilled wells are more close to mountainous area of the river outlet of the upper basin, the GWL is more fluctuated there.

[Please insert Figure 6 here]

[Please insert Figure 7 here]

Figure 8 estimates the total GWL changes for the period of 1981-2010, by considering the crop water requirements, the irrigation use efficiency, the other possible water consumption, and the proportion between the runoff diversion and groundwater extraction, with the decline ranging 0-10m in the irrigation area. The spatial patterns of the changes of GWL are basically consistent with that of net irrigation water requirement, with some significant declines of water table in the

western part of the basin, where the rain-fed ET was lower and more irrigation water was needed.

[Please insert Figure 8 here]

#### 4.4 Future changes

The future mean GWL changes under the four Representative Concentration Pathways (RCP) scenarios, namely RCP2.6, RCP4.5, RCP6.0, and RCP8.5, are shown in Fig. 79. The largest GWL changes for the period of 2017-2050 are predicted to appear in the Linze County with the maximum change value about  $9.36\pm 0.09\text{m}$  (Fig. 9a), indicating the central location of net irrigation water requirement needed would be altered due to future precipitation change and temperature increase compared with the center during the historical period of 1981-2010 in Fig. 8. When the historical GWL changes is added, the total GWL changes during the period of 1981-2050 in Fig. 9b showed that the significant GWL changes (totally 11 grid cells larger than 16 m) would be distributed over the whole farmland belt in MH.

[Please insert Figure 9 here]

The plot in Fig. 10 shows the future uncertainties of ET without irrigation activities for site B. In the scenario of removing irrigation activities from 2017, the GWL would not cease the potential 1.6-1.8 m declining for the future 34 year, i.e. 2017-2050. Referring to the Ganshu Statistics Yearbook (GSY, 2014), the crop production is about 3,256kg/ha for the period of 2000-2013, and the total value is about 4,840 CNY/ha. For Site B, the irrigation area is 3,125 hectare, which creates crop production of 15.13 million CNY/year. To save the 1.6-1.8m decline of GWL, we

need 0.5 billion CNY for the period of 2017-2050 in case we would cease agricultural productions. The total farmland in UHM is about 402,073 hectare. If we remove the agriculture activities from the region, we need to sacrifice 1.9 billion CNY/year, which display a tradeoff between food production and ecology environment protection in the Heihe River.

[Please insert Figure 10 here]

## 5. Conclusions and Discussion

The crop production over the Heihe agricultural region in Northwest China is partly reliant on groundwater. The present study performed a modelling-based analysis by capturing the dominate relationship between groundwater level decline and irrigation water requirement. On the average, about 1.86 m (with the maximum value about 10m) groundwater decline is attributable to irrigation water consumption for the farmland area over the past three decades. Under the future RCP climate scenarios till 2050, in case we cease irrigation activities, the GWL will be prevented to further decline about  $3.06\pm 0.4\text{m}$ , but at the cost of crop production valued  $64.2\pm 8.4$  billion CNY.

The impact of irrigation on groundwater is complicated in MH due to interactions between surface water and groundwater. For example, there is percolation for the irrigated water, and the infiltrated water is further pumped out for irrigation at the lower place along the river. The simulations for all these processes require detailed forcing data and relevant parameters by integrating surface water and groundwater modeling (Zhou et al., 2011; Wu et al., 2014; Tian et al., 2015) and considering

various uncertainties. We avoided the detailed processes at the short timescales, by considering the fact that the depletion of groundwater storage is dominated by the irrigation consumption and constructing a relationship between GWL decline and irrigation water requirement. The irrigation role in groundwater depletion is first quantitatively estimated in Northwest China, for both historical and future periods. The robustness of the model lies in that (1) the runoff generation from both precipitation and snowmelt water in mountain area (UH) was validated by streamflow observations; (2) the evapotranspiration in farmland area was cross-checked with remote sensing data in MH; and (3) the GWL change estimates are basically consistent with the water level evolutions of the observed wells. Certainly, the simplification of only considering the dominant irrigation factor is not comprehensive in modelling GWL dynamics in MH, as observed that the estimated GWL changes are slightly smaller than the observations in Figure 5. The underlying linkage between the irrigation water requirement and groundwater extraction has provided a coherent understanding on the irrigation effects on the regional water cycle, as shown in Figures 4 and 6, and the mean future GWL changes estimated in Figure 7 and a reversing potential in Figure 8 led to new insights on tackling the tradeoff between sustainable agricultural development and ecosystem health. It is noted that we did not include future land use/land cover changes which affects GWL changes in present study, as we had no clear clues to design reasonable scenarios on land use/land cover changes.

The irrigation activities have caused about 1.86m groundwater decline in MH for

the past three decades, and may be worrisome in the future with a further  $3.06\pm 0.4\text{m}$  decline till 2050. If that happened, the difficulties of regional water supply would be aggravated, resulting in lower irrigation efficiency and unsustainable agricultural production. The lower groundwater level will also affect the surrounding grasslands and forest with decreasing vegetation cover and correspondingly threatening fragile ecological systems in arid regions.

The annual water budget over a  $9,097\text{ km}^2$  irrigation area in MH for the period of 2000-2008 were estimated by Wu et al. (2014). The inflow and precipitation were 2.48 and 1.23 billion  $\text{m}^3/\text{year}$ ; the ET and runoff were 2.82 and 1.08 billion  $\text{m}^3/\text{year}$ , and the pumping was 0.34 billion  $\text{m}^3/\text{year}$  (Figure 5 in Wu et al., 2014). From the present study, rain-fed ET for this area is about 69% of irrigated ET. According to the above water budget, if we cease irrigation by stopping pumping, the amount of water saved ( $2.48+1.23-2.82\times 0.69-1.08=0.685$  billion  $\text{m}^3/\text{year}$ ) can elevate the water level by 0.075 m/year. For the decreased groundwater level of 1.9m of the same region during the period of 1981-2010, it would take about 25 year to recover under the average climate during 2000-2008. Ceasing irrigation can certainly reverse the decline trend of groundwater level, however this will never happen due to the demand for food production. The other feasible options are (1) to breed drought tolerant cultivars, which can maintain or even increase crop yield with less irrigation; (2) to increase crop water productivity by adopting advanced water-saving measures, agronomic practices (Li et al., 2017), and regional vulnerability information; (3) to alter cropping patterns, by increasing rain-fed area and reducing reliance to groundwater (Grogan et

al., 2015); and (4) possible water transfer projects.

One limitation of this study is that we did not highlight the environment consequence, such as the vegetation dynamics, of the continuing underground water extraction for the studied area. It is more favorable to quantify the critical value and provide the recommended groundwater levels. To study the relationships between vegetation dynamics and the real groundwater level, more detailed and continuous data are required, and which is our next step for future research.

### **Acknowledgements**

This work was financially supported by the National Natural Science Foundation of China (51679233, 91425302), the National Key Research and Development Plan (2016YFC0400207), the Special Fund for Agro-scientific Research in the Public Interest (201503125), and the Programme of Introducing Talents of Discipline to Universities (B14002). We thank Dr. Benedito Albuquerque da Silva and the two anonymous reviewers for their constructive comments and useful suggestions which resulted in a far more accurate presentation of our work.

## References

- Calow, R.C., Howarth, S.E., Wang, J., 2009. Irrigation development and water rights reform in China. *Int. J. Water Resour. Dev.* 25, 227–248.
- Cao, G., Zheng, C., Scanlon, B.R., Liu, J., Li, W., 2013. Use of flow modeling to assess sustainability of groundwater resources in the North China Plain. *Water Resour. Res.* 49, 159–75.
- Chen, Y.Y., Niu, J., Kang, S.Z., Zhang, X.T., 2018. Effects of irrigation on water and energy balances in the Heihe River basin using VIC model under different irrigation scenarios. *Sci. Total Environ.* 645, 1183 – 1193.
- Collins, W.J., et al., 2008. Evaluation of the HadGEM2 model. Met Office Hadley Centre Technical Note no. HCTN 74, available from Met Office, FitzRoy Road, Exeter EX1 3PB.
- Currell, M., Han, D., Chen, Z., Cartwright, I., 2012. Sustainability of groundwater usage in northern China: dependence on paleowaters and effects on water quality, quantity, and eco-system health. *Hydrol. Process.* 26, 4050–66.
- Famiglietti, J.S., Lo, M., Ho, S.L., Bethune, J., Anderson, K.J., Syed, T.H., Swenson, S.C., de Linage, C.R., Rodell, M., 2011. Satellites measure recent rates of groundwater depletion in California's Central Valley. *Geophys. Res. Lett.* 38, L03403.FAO, 2013. AQUASTAT: FAO's Information System on Water and Agriculture. Food and Agriculture Organization of the United Nations, Rome, Italy.
- FAO, 2017. The Future of Food and Agriculture - Trends and challenges, Rome.
- Feng, W., Zhong, M., Lemoine, J.M., Biancale, R., Hsu, H.T., Xia, J. 2013. Evaluation of groundwater depletion in North China using the Gravity Recovery and Climate Experiment

- (GRACE) data and ground-based measurements. *Water Resour. Res.* 49, 2110–2118.
- Frenken, I., Gillet, V., 2012. Irrigation water requirement and water withdrawal by country. AQUASTAT, Food and Agricultural Organization of the United Nations, P.264.
- Gansu Statistical Yearbook (GSY), 2014. Gansu Province Bureau of Statistics, [www.gstj.gov.cn](http://www.gstj.gov.cn).
- Grogan, D.S., Zhang, F., Prusevich, A., Lammers, R.B., Wisser, D., Glidden, S. Li, C., Froking, S., 2015. Quantifying the link between crop production and mined groundwater irrigation in China. *Sci. Total Environ.* 511, 161–175.
- Haddeland, I., Lettenmaier, D.P., Skaugen, T., 2006. Effects of irrigation on the water and energy balances of the Colorado and Mekong river basins. *J. Hydrol.* 324, 210–223.
- Kang, S.Z., Su, X.L., Tong, L., Shi, P.Z., Yang, X.Y., Abe, Y.K., Du, T.S., Shen, Q.L., Zhang, J.H., 2004. The impacts of human activities on the water-land environment of the Shiyang River basin, an arid region in northwest China. *Hydrolog. Sci. J.* 49, 413–427.
- Lakshmi, V., Piechota, T., Narayan, U., Tang, C. 2004. Soil moisture as an indicator of weather extremes. *Geophys. Res. Lett.* 31, L11401, doi:10.1029/2004GL019930.
- Li, X.L., Tong, L., Niu, J., Kang, S.Z., Du, T.S., Li, S.E., Ding, R.S., 2017. Spatio-temporal distribution of irrigation water productivity and its driving factors for cereal crops in Hexi Corridor, Northwest China. *Agr. Water Manage.* 179, 55–63.
- Liang, X., Lettenmaier, D.P., Wood, E.F., Burges, S.J., 1994. A simple hydrologically based model of land surface water and energy fluxes for general circulation models. *J. Geophys. Res.* 99, 14415–14428.
- Lohmann, D., Nolte-Holube, R., Raschke, E., 1996. A large scale horizontal routing model to be coupled to land surface parameterization schemes. *Tellus* 48, 708–721.

- Molden, D., et al., 2007. Trends in water and agricultural development. In: Molden, D. (Ed.). *Water for food, water for life: A Comprehensive assessment of water management in agriculture*. Earthscan Publications. Colombo, Sri Lanka: London. IWMI, pp. 57–89.
- Nijssen, B., Schnur, R., Lettenmaier, D.P., 2001. Global retrospective estimation of soil moisture using the variable infiltration capacity land surface model, 1980–1993. *J. Climate* 14, 1790–1808.
- Portmann, F.T., Siebert, S., Doell, P., 2010. MIRCA2000 — global monthly irrigated and rainfed crop areas around the year 2000: a new high-resolution data set for agricultural and hydrological modeling. *Global Biogeochem. Cy.* 24, GB1011.
- Rodell, M., Velicogna, I., Famiglietti, J.S., 2009. Satellite-based estimates of groundwater depletion in India. *Nature* 460, 999–1002.
- Scanlon, B.R., Faunt, C.C., Longuevergne, L., Reedy, R.C., Alley, W.M., McGuire, V.L., McMahon, P.B., 2012. Groundwater depletion and sustainability of irrigation in the US High Plains and Central Valley. *Proc. Natl. Acad. Sci. USA* 109, 9320–9325.
- Shiklomanov, I.A., Rodda, J.C., 2003. *World Water Resources at the Beginning of the 21st Century*, UNESCO International Hydrology Press Ed. Cambridge University Press.
- Shuttleworth, W.J., 1993. Evaporation. In: Maidment, D.R. (Ed.), *Handbook of Hydrology*. McGraw-Hill, New York, pp. 4.1–4.53.
- Tatsumi, K., Yamashiki, Y., da Silva, R.V., Takara, K., Matsuoka, Y., Takahashi, K., Maryyama, K., Kawahara, N., 2011. Estimation of potential changes in cereals productions under climate change scenarios. *Hydrol. Process.* 25, 2715–2725.
- Tatsumi, K., Yamashiki, Y., 2015. Effect of irrigation water withdrawals on water and energy

- balance in the Mekong River Basin using an improved VIC land surface model with fewer calibration parameters. *Agric. Water Manage.* 159, 92–106.
- Tian, Y., Zhen, Y., Zheng, C.M., Xiao, H.L., Fan, W.J., Zou, S.B., Wu, B., Yao, Y.Y., Zhang, A.J., Liu, J., 2015. Exploring scale-dependent ecohydrological responses in a large endorheic river basin through integrated surface water-groundwater modeling. *Water Resour. Res.* 51, 4065–4085.
- Shi, Y., Eberhart, R. C., 1998. Parameter selection in particle swarm optimization. In *Proceedings of 7th conference on evolutionary programming VII*, pp. 591–600. Berlin: Springer.
- Todini, E., 1996. The ARNO rainfall-runoff model. *J. Hydrol.* 175, 339–382.
- Wu, B., Zheng, Y., Tian, Y., Wu, X., Yao, Y.Y., Han, F., Liu, J., Zheng, C.M., 2014. Systematic assessment of the uncertainty in integrated surface water-groundwater modeling based on the probabilistic collocation method. *Water Resour. Res.* 50, 5848–5865.
- Wu, Y.P., Liu, S.G., Young, C.J., Dahal, D., Sohl, T.L., Davis, B., 2015. Projection of corn production and stover-harvesting impacts on soil organic carbon dynamics in the U.S. Temperate Prairies. *Sci. Rep.* 5, 10830, doi: 10.1038/srep10830.
- Xiong, Z., Yan, X., 2013. Building a high-resolution regional climate model for the Heihe River Basin and simulating precipitation over this region. *Chin. Sci. Bull.*, 58(36), 4670–4678.
- You, L.Z., Xie, H., Guo, Z., Wang, L., 2014. Irrigation potential and investment return in Kenya. *Food Policy* 47, 34–45.
- Zhangye-MY, 2010. *Zhangye Management Yearbook*, Zhangye Water Affairs Office 1991-2010.
- Zhao, R.J., Zhang, Y.L., Fang, L.R., Liu, X.R., Zhang, Q.S., 1980. The Xinanjiang model. In *Hydrological Forecasting*, IAHS Publ., No.129. IAHS Press: Wallingford, 351–356.

Zhou, J., Hu, B.X., Cheng, G.D., Wang, G.X., Li, X., 2011. Development of a three-dimensional watershed modelling system for water cycle in the middle part of the Heihe rivershed, in the west of China. *Hydrol. Process.* 25, 1964–1978.

Zou, M.Z., Kang, S.Z., Niu, J., Lu, H.N., 2018. A new technique to estimate regional irrigation water demand and driving factor effects using an improved SWAT model with LMDI factor decomposition in an arid basin. *J. Clean. Prod.* 185, 814 – 824.

## Figure captions

**Figure 1.** Location of the study area and the irrigation-related details. (a) The Heihe River basin in Northwest China, and the study domain of the upper and middle reaches (UMH). (b) The land use and weather/gauging stations in UMH. (c) Average rain-fed evapotranspiration. (d) Average free-irrigated evapotranspiration simulated by the VIC model. (e) The derived net irrigation water requirement for the period of 1980-2010. (f) The aqueducts and monitoring wells in Linze and Ganzhou Counties.

**Figure 2.** The frame diagram of the proposed study.

**Figure 3.** Comparison between the observed and simulated streamflow at Yingluoxia station for (a) calibration (1986-1991) and (b) validation (1993-1999) periods.

**Figure 4.** Comparison of monthly grid ET simulation by the VIC model and the derived data from remote sensing products at grid cell (a) Site C and (b) Site D.

**Figure 5.** The simulated monthly evapotranspiration evolutions for the free-irrigated and rain-fed situations with the corresponding ground level changes derived for Site A along the time. Site A is marked in Figure 1(b).

**Figure 6.** The observed and inverted groundwater levels. (a) The observed groundwater level of 9 wells in Linze District for the period 1990-2004 (left panel), and the average value of the inverted groundwater level changes estimated for the district, marked as bold red line, with observed changes of 15 observed wells (right panel). (b) Same as (a) but for Ganzhou District.

**Figure 7.** The observed and inverted groundwater levels. (a) The observed groundwater level of 9 wells in Linze District for the period 2000-2010 (left panel), and the average value of the inverted groundwater level changes estimated for the district, marked as bold red line, with observed changes of 10 observed wells (right panel). (b) Same as (a) but for Ganzhou District.

**Figure 8.** The estimated GWL changes for the period of 1981-2010. GWL refer to groundwater level.

**Figure 9.** Spatial distribution of GWL changes. (a) Mean GWL changes derived by inverting method based on modified VIC model simulation and relevant water allocation data

under four RCP scenarios (RCP2.6, RCP4.5, RCP6.0, and RCP8.5). (b) Total estimated GWL changes for the period of 1981-2050, in which the RCP-based mean value is used for future period.

**Figure 10.** The future GWL changes with the situation of no irrigation under four RCP scenarios (RCP2.6, RCP4.5, RCP6.0, and RCP8.5) for one selected grid cell Site B. Site B is marked in Figure 1(b).

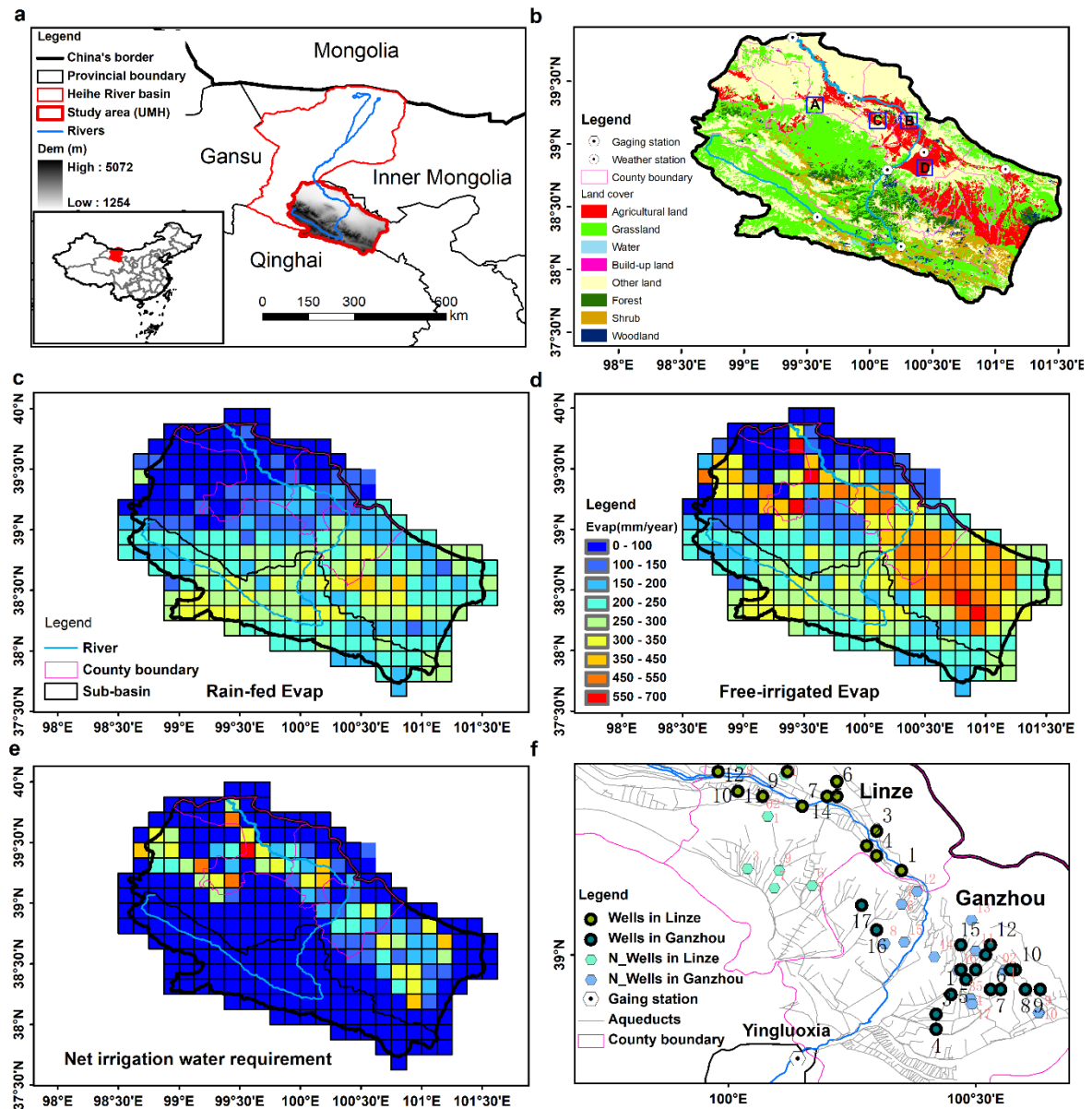


**Figure 1.** Location of the study area and the irrigation-related details. (a) The Heihe River basin in Northwest China, and the study domain of the upper and middle reaches (UMH). (b) The land use and weather/gauging stations in UMH. (c) Average rain-fed evapotranspiration. (d) Average free-irrigated evapotranspiration simulated by the VIC model. (e) The derived net irrigation water requirement for the period of 1980-2010. (f) The aqueducts and monitoring wells in Linze and Ganzhou Counties.

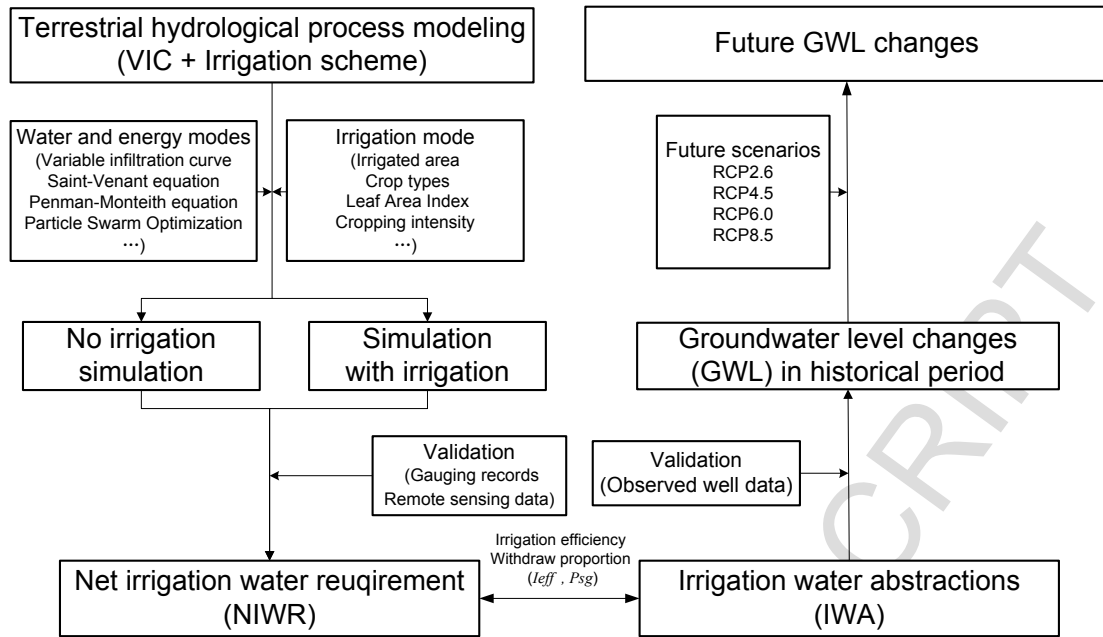


**Figure 2.** The frame diagram of the proposed study.

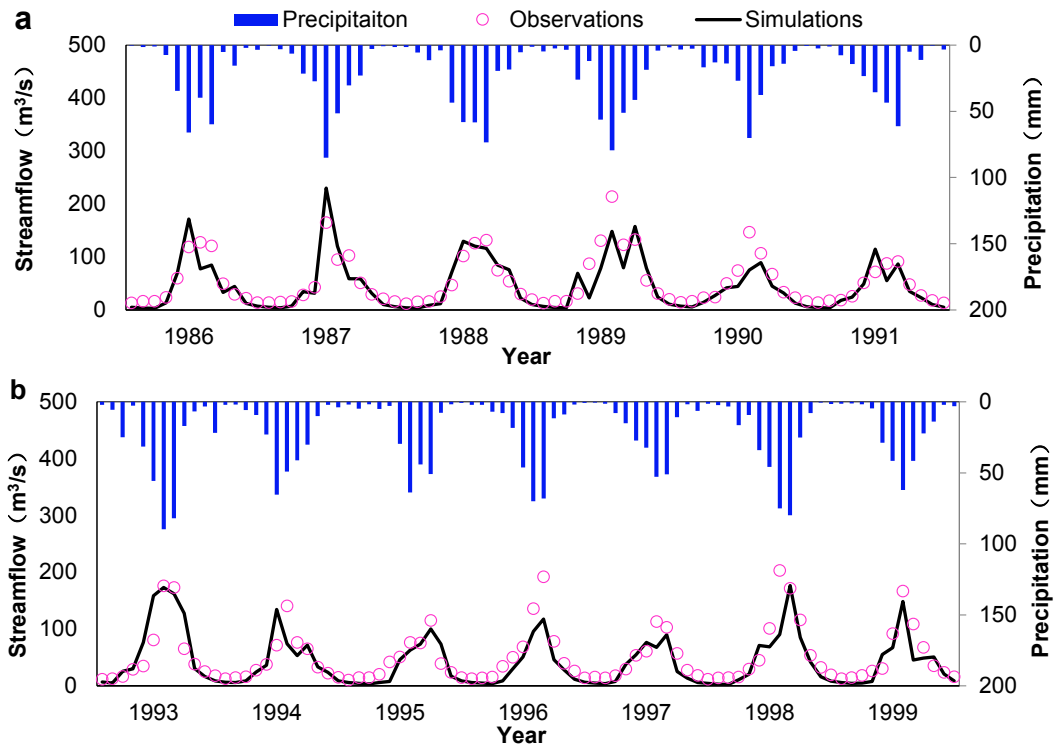


**Figure 3.** Comparison between the observed and the VIC simulated streamflow at the Yingluoxia station for (a) calibration (1986-1991) and (b) validation (1993-1999) periods.

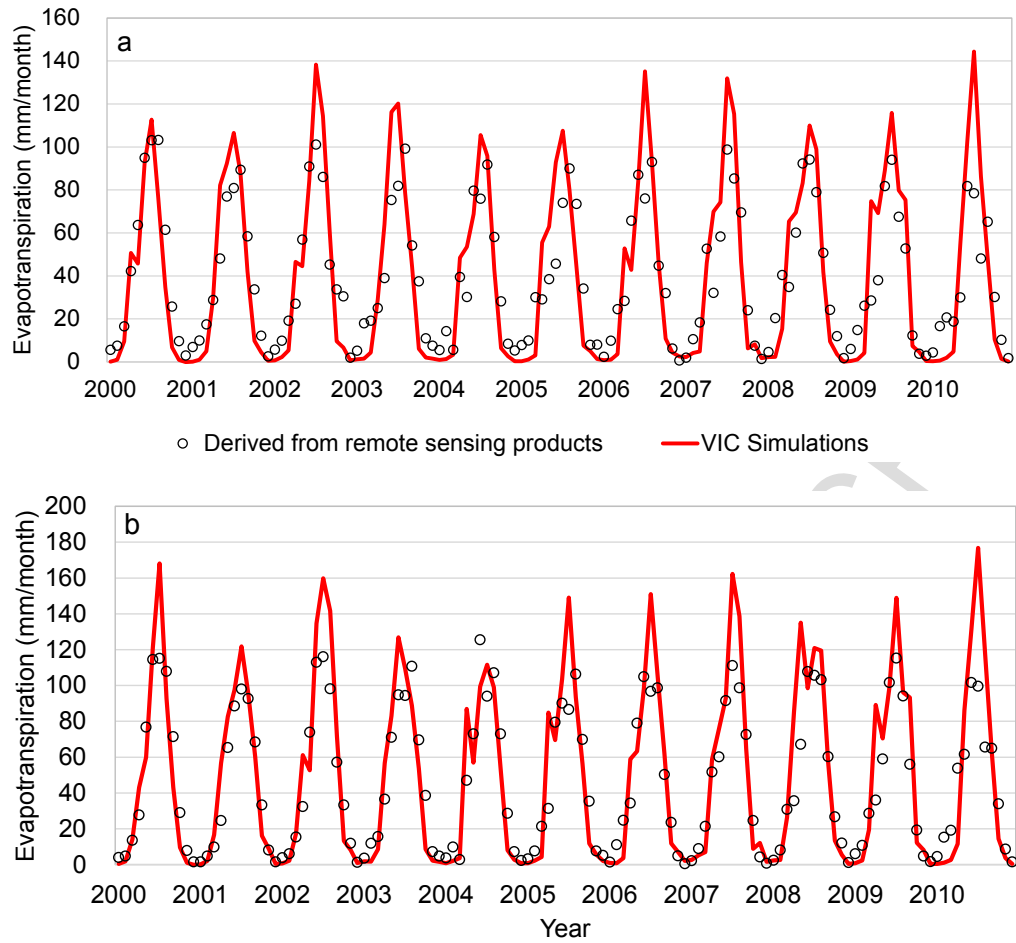


**Figure 4.** Comparison of monthly grid ET simulation by the VIC model and the derived data from remote sensing products at grid cell (a) Site C and (b) Site D.

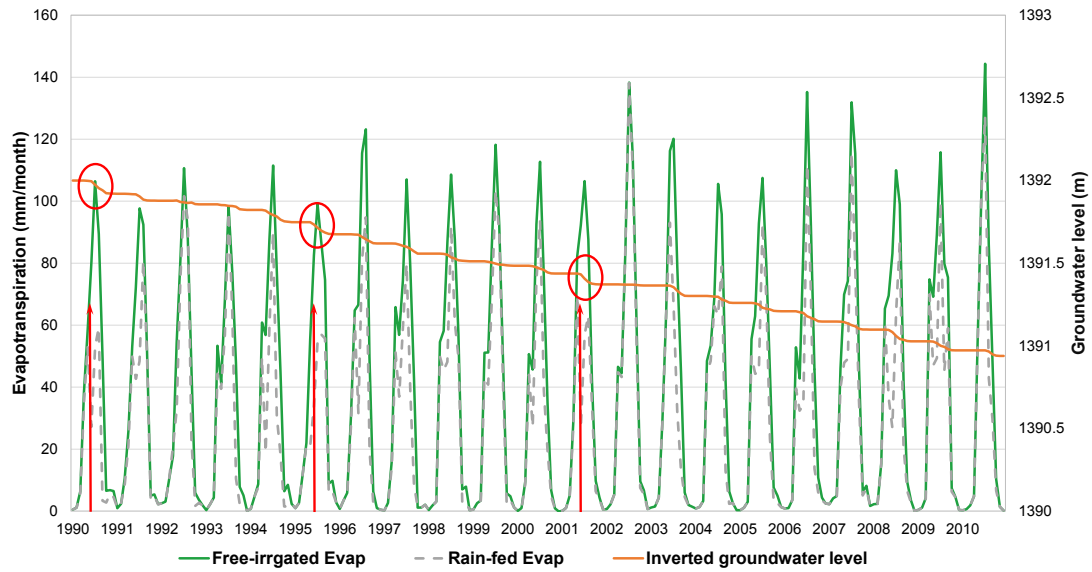


**Figure 5.** The simulated monthly evapotranspiration evolutions for the free-irrigated and rain-fed situations with the corresponding ground level changes derived for Site A along the time. Site A is marked in Figure 1(b).

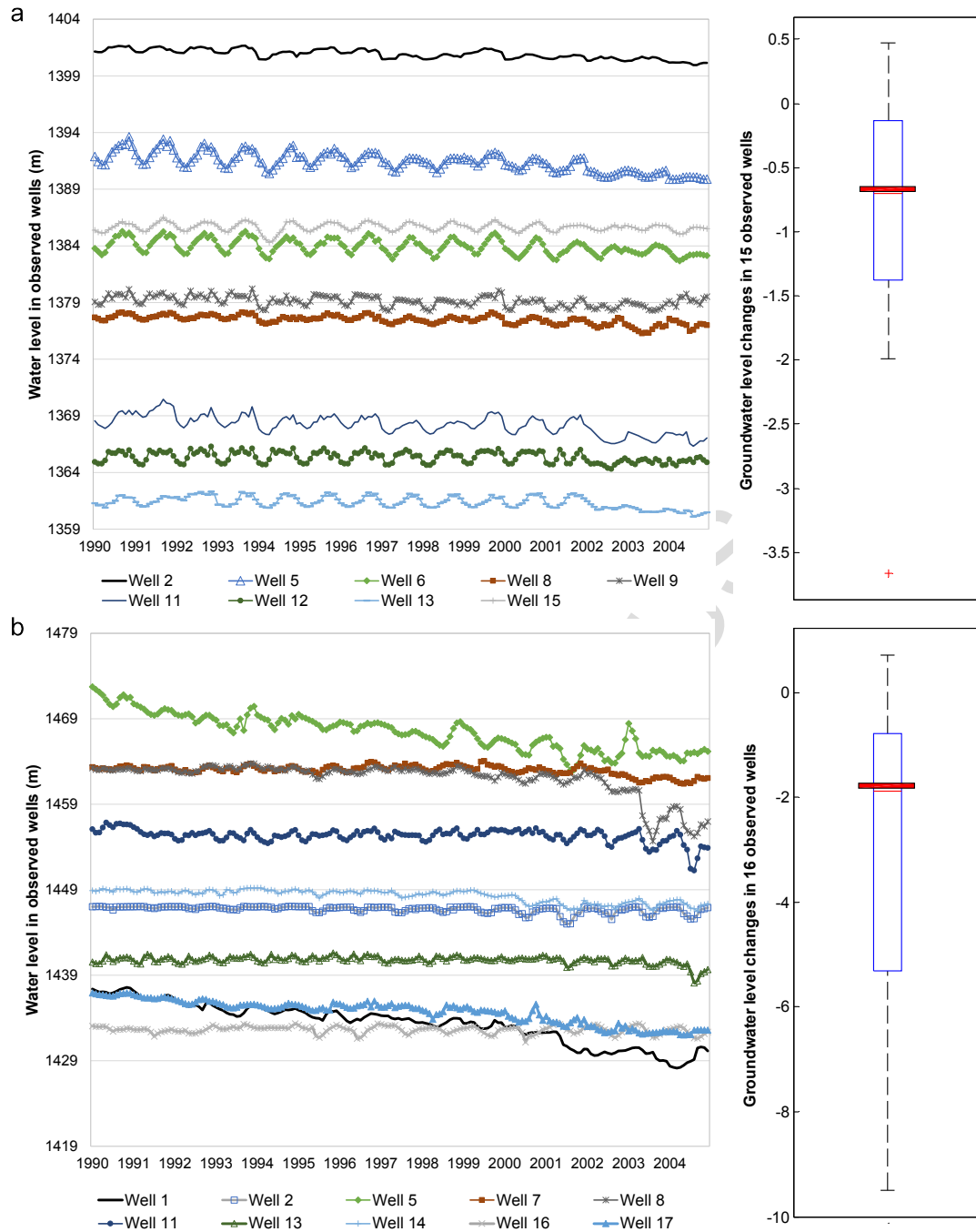


**Figure 6.** The observed and inverted groundwater levels. (a) The observed groundwater level of 9 wells in Linze District for the period 1990-2004 (left panel), and the average value of the inverted groundwater level changes estimated for the district, marked as bold red line, with observed changes of 15 observed wells (right panel). (b) Same as (a) but for Ganzhou District.

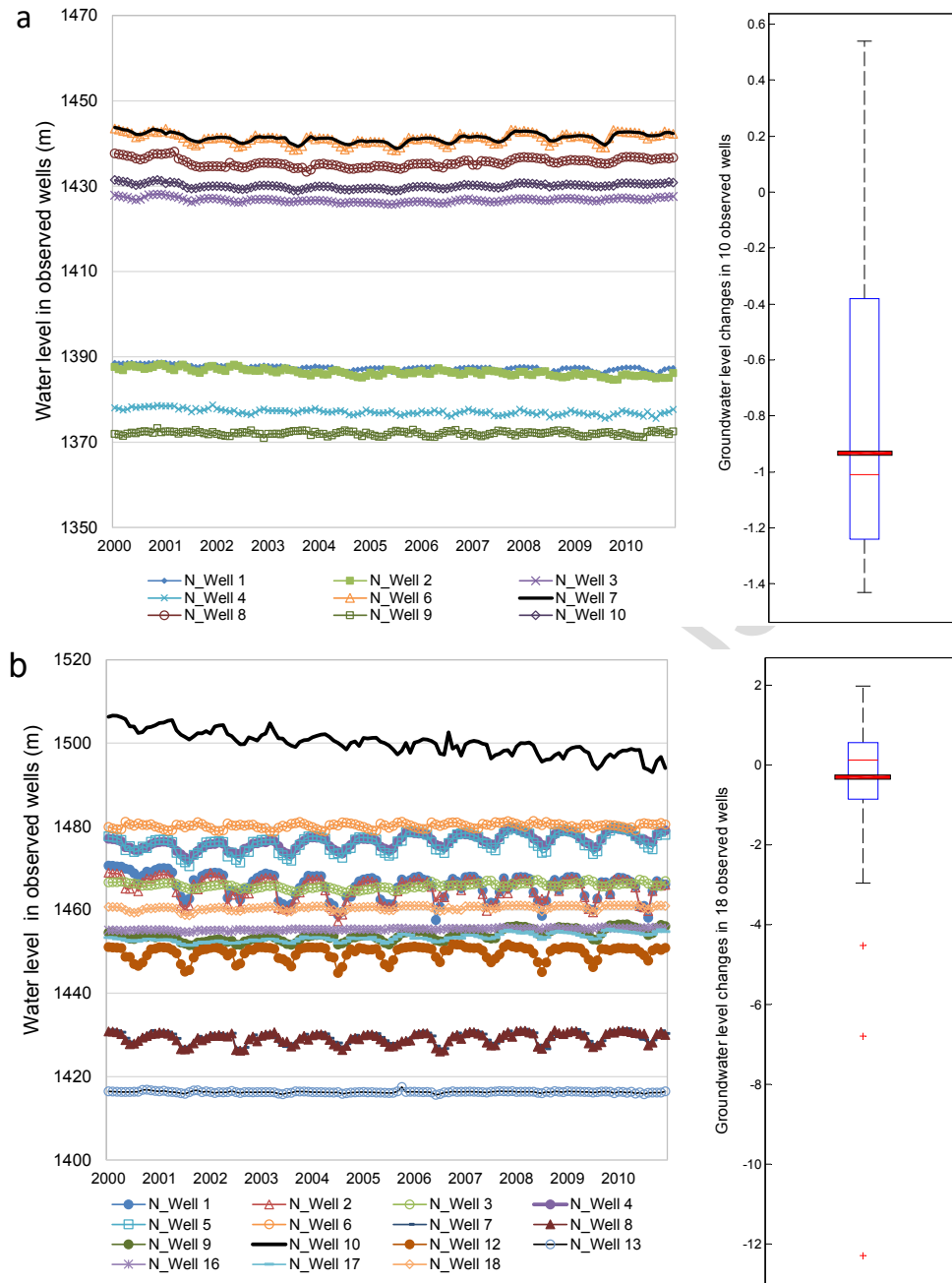


**Figure 7.** The observed and inverted groundwater levels. (a) The observed groundwater level of 9 wells in Linze District for the period 2000-2010 (left panel), and the average value of the inverted groundwater level changes estimated for the district, marked as bold red line, with observed changes of 10 observed wells (right panel). (b) Same as (a) but for Ganzhou District.

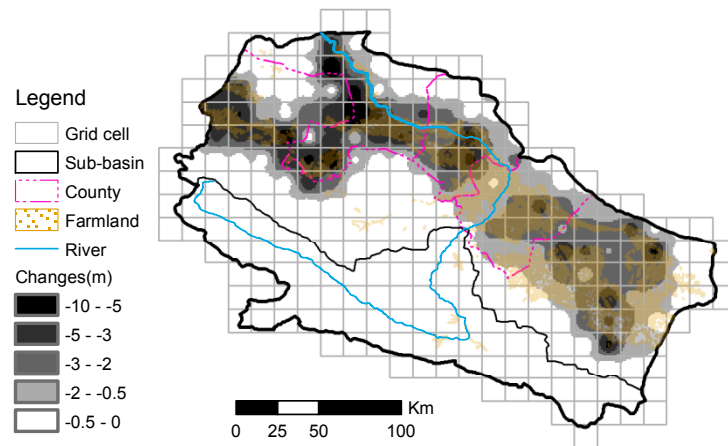


**Figure 8.** The estimated GWL changes for the period of 1981-2010. GWL refer to groundwater level.

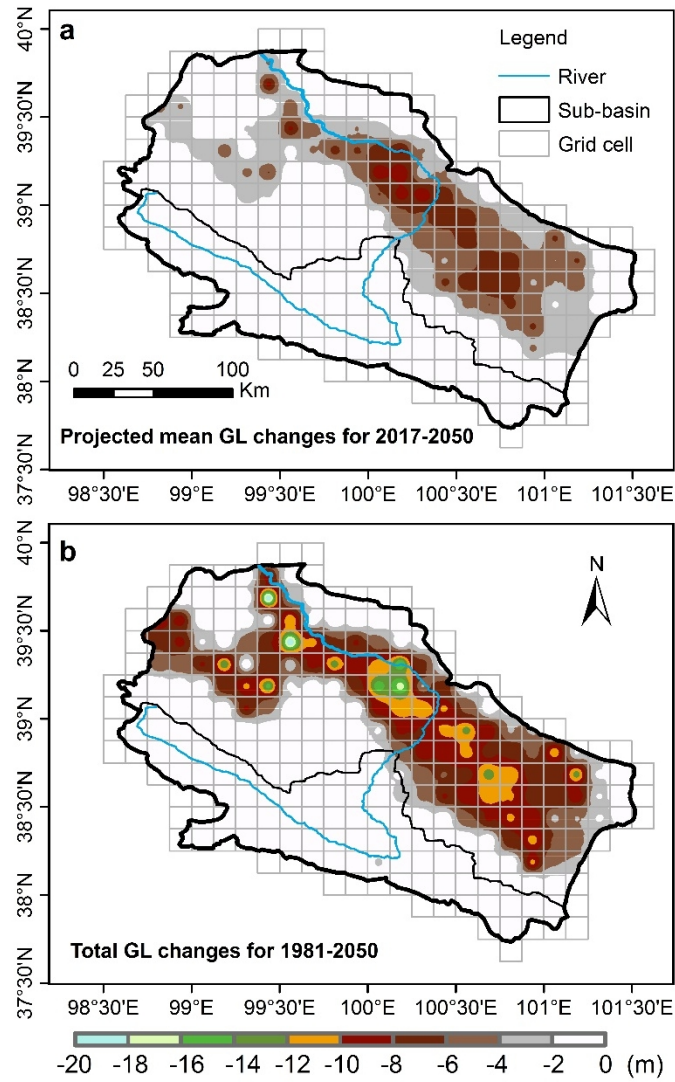


**Figure 9.** Spatial distribution of GWL changes. (a) Mean GWL changes derived by inverting method based on modified VIC model simulation and relevant water allocation data under four RCP scenarios (RCP2.6, RCP4.5, RCP6.0, and RCP8.5). (b) Total estimated GWL changes for the period of 1981-2050, in which the RCP-based mean value is used for future period.

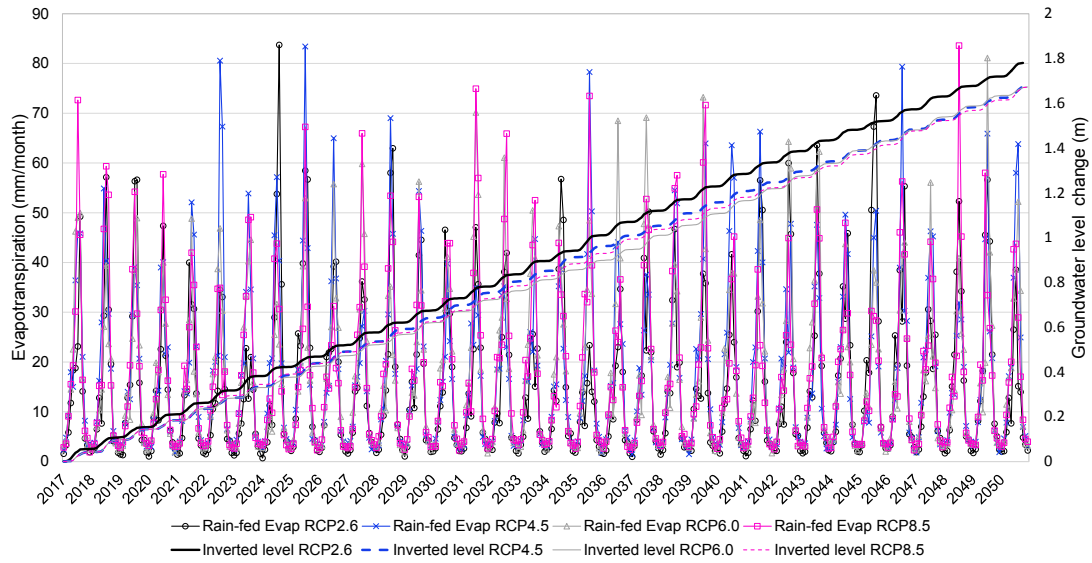


**Figure 10.** The future GWL changes with the situation of no irrigation under four RCP scenarios (RCP2.6, RCP4.5, RCP6.0, and RCP8.5) for one selected grid cell Site B. Site B is marked in Figure 1(b).

**Highlights:**

- The production sustainability on irrigation water in the Heihe Oasis are assessed
- The groundwater level (GWL) declines attributed to crop production are examined
- The cost we need to pay for ceasing GWL declines in farmland region is quantified